NATIONAL BOARD FOR TECHNICAL EDUCATION
NIGERIAN JOURNAL FOR TECHNICAL EDUCATION
Volume 21 Nos. 1 2023
ISSN No. 2992 - 3522

Performance Analysis of Two-phase Induction Motor Operating with Symmetrical Windings Using MATLAB/Simulink

Ekpo, Edet George[1] and Gideon. D. Umoh[2]
[1]Department of Electrical Electronics Engineering, AkwaIbom State Polytechnic, IkotOsurua. georgeekpo@gmail.com
[2]Department of Electrical Electronics Engineering Maritime Academy of Nigeria, Oron.

Abstract:
This research models and simulates a symmetrical wound Two-Phase Induction Motor (TPIM). The winding arrangement is obtained by making both the phase winding of main and auxiliary of the Motor equal in turns, properties, and connected to a Two-Phase Power Supply. The Power Supply is obtained from an inverter with source either from batteries or a rectified power supply. The Motor Models are based on induction motor mathematical expressions, geometric dimension and implemented using MATLAB/Simulink Program. The current, torque and speed wave forms under no-load and full-load conditions were compared with that of a Capacitor-Start Capacitor-Run Single-Phase Induction Motor (CSCR-SPIM); the transient and steady state performance were analyzed. The simulation models created in MATLAB/Simulink were also compared with laboratory measurements, and the results showed that the modeled machine is advantageous in its operation as compared to a Poly-Phase Induction Motor. The two-phase induction motor also has characteristic similar to three-phase induction motor such; heavy starting torque, improved power factor, minimized torque harmonics and increased power rating.

Keywords: Single-Phase Induction Motor, Two Phase Induction Motor, Three-Phase Induction Motor, Symmetrical Winding, Matlab/Simulink

1. Introduction

Induction machine has found great relevance commercially and industrially due to the robustness, simplicity and cost-effectiveness (Naser, A. 2002). It is commonly divided into two main categories such as Single-Phase Induction Machine (SPIM) and Three-Phase Induction Machine (3PIM). SPIM are widely domesticated, even though it found it applicability in agriculture and some industrial applications. Most household appliance and some production machines such as microwave cookers, grinders etc are equipped with single-phase induction motor.

SPIM have an elliptic air gap magnetic field due to the asymmetric of stator configuration of the main and auxiliary windings (Naser, A. 2002 & Sobhan, S. 2013). Due to the elliptic nature of the rotating field, creating a forward and backward field, a braking torque is created by the backward field, and thus, additional loss to the machine and torque. Such field is a source of noise and vibrations (Hraboveova, V. 2010).

Though the capacitor start induction machine is self-starting as well as having an

enhance running performance, it records disadvantages which can be overcome by centrifugally disconnecting the capacitor before the motor reaches it maximum operating speed (Mera, R. 2012). A start-capacitor connected in series with the auxiliary winding is typically to blame for the voltage time shift in the auxiliary winding.

The run-capacitor only increased the machine's efficiency in the air gap with an elliptic magnetic field (Sobhan, S. 2013).

It is necessary to continuously change the capacitance value in order to improve SPIM performance across the whole speed range provided by these capacitor switches. (Huang, H. 1988).

Therefore, when the rated power exceeds 0.5 kW, using a single-phase induction motor is not financially viable. (Fushs, E. 1990). Comparatively, CSCR-SPIM efficiency thus is greater than the permanent connected start-capacitor motor; it is less than three-phase induction motor of the same capacity. Three-phase symmetrical voltage is used to power three-phase induction machines.

And it stator's windings are mutually offset by 120 electrical degrees (Zhou, P. 1999).

Circular magnetic fields are used by these machines to operate,, revolving at a synchronous speed and exhibited heavy starting torque, improved power factor and efficiency, less torque harmonics and higher rated power to drive load.

Many researchers had investigated greatly on efficiency improvement of single-phase induction motors; (Xinhua, L. 2001) proposed a novel energy efficient single-phase induction motor, which has three series-connected windings and two capacitors, which make a three-phase induction motor operate from single-phase power supply. In order to control the VSI to mimic a dynamic capacitor for low cost open loop control of SPIM, (Vishal, V. 2008) describes a new indirect current control approach.

The resulting dynamic capacitance utilizes all of the machine's available torque. The proposed indirect current control scheme can easily be attached to already existing system without modification in the equipment.
For a maximum torque, an indirect current control voltage Source Inverter (VSI) is employed to ensure that the phase quadratures between the windings current are maintained.

SPIM can be rearranged to have two-phase windings in its stator slots (i.e. a winding layout with two symmetric and orthogonal phase-windings), where both windings exhibiting same characteristics (Sorrentino, E. 2011). And if powered by two-phase power supply which is spatially space by 90 electrical degree, the machine operate with a circular magnetic field revolving at synchronous speed and exhibit characteristic similar to a 3PIM of the same capacity thus vibrations and unfavorable noise are suppressed. As with the use of a suitable controller, the 2-phase supplied can be obtained from the line (Van der Merwe, C. 1995). This paper presents the Performance Analysis of Two-phase Induction Machine Operating with Symmetrical Windings Using MATLAB/Simulink. This numerical method is more suitable for the electromagnetic field analysis of electric machines; such as complex geometries, magnetic and electric circuit, and induced currents, coupling of flux and mechanical response (Salon, S. 1995 & Vassent, E. 1991).

2. Mathematical Model

The 2-phase induction motor (TPIM) is modeled to be orthogonal as shown in fig.1. The windings have a sinusoidal waveform resulting from the arrangement of the windings in the slots. The stationary a-b axes may be aligned with the orthogonal axes of the physical winding as shown in Fig 1.

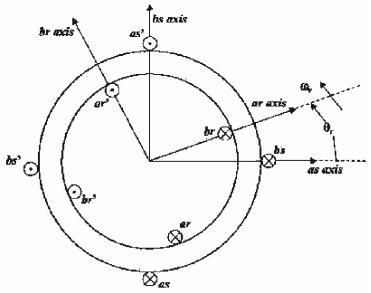

Figure 1: Cross-sectional view of TPIM arranged in space quadrature.

The mathematical model describing the operation of electrical machines describes the effect of the time varying electromagnetic field. In addition, the circuit equations accommodate the voltage equations and the torque equations of the machine.

The voltage and torque equations expressed in machine variables may be obtained byfollowing the procedure used for the 3-phase machine. The voltage of each phase, v_a and v_b for stator and rotor within the induction machine can be written as;

$$v_{as} = r_a i_{as} + p\lambda_{as} \quad \text{.....2.1}$$
$$v_{bs} = r_b i_{bs} + p\lambda_{bs} \quad \text{.....2.2}$$
$$v_{ar} = r_r i_{ar} + p\lambda_{ar} \quad \text{.....2.3}$$
$$v_{br} = r_r i_{br} + p\lambda_{br} \quad \text{.....2.4}$$

The ρ is$\left(\frac{d}{dt}\right)$

The flux linkage equations of the stator and rotor

$$\begin{bmatrix}\lambda_{abs}\\ \lambda_{abr}\end{bmatrix} = \begin{bmatrix} L_s & L_{sr} \\ (L_{sr})^T & L_r \end{bmatrix}\begin{bmatrix} i_{abs} \\ i_{abr}\end{bmatrix} \quad \text{.....2.5}$$

Where

$$L_s = \begin{bmatrix} L_{asas} & L_{asbs} \\ L_{bsas} & L_{bsbs}\end{bmatrix} + \begin{bmatrix} L_{las} & 0 \\ 0 & L_{lbs}\end{bmatrix} \quad \text{.....2.6}$$

$$L_r = \begin{bmatrix} L_{arar} & L_{arbr} \\ L_{brar} & L_{brbr}\end{bmatrix} + \begin{bmatrix} L_{lar} & 0 \\ 0 & L_{lbr}\end{bmatrix} \quad \text{.....2.7}$$

$$L_{sr} = \begin{bmatrix} L_{asar} & L_{asbr} \\ L_{bsar} & L_{bsbr}\end{bmatrix} \quad \text{.....2.8}$$

$$V = IR + \frac{d}{dt}[LI]; where\lambda = [LI] \quad \text{.....2.9}$$

$$wherew_r = \frac{d\theta}{dt}; R = diag[r_{as}, r_{bs}, r_{ar}, r_{br}];$$

$$V = \begin{bmatrix} V_{as} \\ V_{bs} \\ 0 \\ 0\end{bmatrix}; I = \begin{bmatrix} i_{as} \\ i_{bs} \\ i_{ar} \\ i_{br}\end{bmatrix}; L = \begin{bmatrix} (L_{asas} + L_{ls}) & L_{asbs} & L_{asar} & L_{asbr} \\ L_{bsas} & (L_{bsbs} + L_{lS}) & L_{bsar} & L_{bsbr} \\ L_{aras} & L_{arbs} & (L_{arar} + L_{lr}) & L_{arbr} \\ L_{bras} & L_{brbs} & L_{brar} & (L_{brbr} + L_{lR}\end{bmatrix}$$

The Leakage inductances of stator windings isL_{ls} while that of the rotor windings is L_{lr} .

The torque equation for the motor is expressed as:

$$T_e = (P/2)(i_{abs})^T \frac{d}{d\theta_r}\begin{bmatrix} L_{sr}\cos(\theta_r) & -L_{sr}\sin(\theta_r) \\ L_{Sr}\sin(\theta_r) & L_{Sr}\cos(\theta_r)\end{bmatrix} i_{abr} \quad \text{.....2.10}$$

Expanding equation 2.10 yields equation 2.11;

$$T_e = ({}^{P}/_{2})L_{sr}i_{as}(-i_{ar}\sin(\theta_r) - i_{br}\cos(\theta_r)) + L_{Sr}i_{bs}(i_{ar}\cos(\theta_r) - i_{br}\sin(\theta_r)) \quad \text{.....2.11}$$

The inductance L_{sr} is the modulus of the mutual inductances between stator and rotor.
The relationship between the speed and torque is given in equation 2.12.

$$T_e = J\left(\frac{2}{P}\right)\frac{d}{d\theta_r}Pw_r + T_L \quad \text{.....2.12}$$

3. Inductance Calculations

For the induction calculations, the winding function method [14], can be employed, as presented in equation 2.13.

$$L_{xy} = \mu_0 rl\int_0^{2\pi} N_a(\varphi)N_b(\varphi)gp^{-1}(\varphi,\theta_r)d\varphi \quad \text{.....2.13}$$

Where $N_a(\varphi)$ and $N_b(\varphi)$ are the winding functions of the Main and the Auxiliary phase respectively and φ is the stator circumferential position. $gp^{-1}(\varphi,\theta_r)$is the inverse air gap function.[14].

$$gp^{-1}(\emptyset_s,\theta_r) = a - bcos2(\emptyset_s - \theta_r) + \frac{b}{3}cos6(\emptyset_s - \theta_r) \quad \text{.....2.14}$$

Where,

$$a = \frac{1}{2}\left(\frac{1}{g_1} + \frac{1}{g_2}\right) \quad \text{.....2.15}$$

$$b = \frac{2}{\pi}\left(\frac{1}{g_1} - \frac{1}{g_2}\right)sin\pi\beta \quad \text{.....2.16}$$

Where g_1 is the main air gap length, g_2 is the inter-polar slot space and β is the ratio of pole arc to slot pitch.

For self-inductances, equation (17) will be of the form of (13):

$$L_{xx} = \mu_0 rl\int_0^{2\pi}[N_x(\varphi)]^2 gp^{-1}(\varphi,\theta_r)d\varphi \quad \text{.....2.17}$$

The fundamental components of the winding functions for the stator and rotor windings are given as;

$$N_{as} = N_A\cos(\varphi), \qquad N_{bs} = N_B\cos(\varphi) \quad \text{.....2.18}$$

$$N_{ar} = N_r\cos(\varphi - \varphi_r), \qquad N_{br} = N_r\cos(\varphi - \varphi_r) \quad \text{.....2.19}$$

The machine inductances are presented in equation 2.20 to equation 2.31.

$$L_{asas} = \frac{\mu_0 rl}{gp}\int_0^{2\pi}(N_A\cos(\varphi))^2 d\varphi = \frac{\mu_0 rl}{gp}\pi N_A^2 \quad \text{.....2.20}$$

$$L_{asbs} = \frac{\mu_0 rl}{gp}\int_0^{2\pi} N_A\cos(\varphi) \times N_B\sin(\varphi)\, d\varphi = 0 \quad \text{.....2.21}$$

$$L_{bsas} = \frac{\mu_0 rl}{gp}\int_0^{2\pi} N_B\sin(\varphi) \times N_A\cos(\varphi)\, d\varphi = 0 \quad \text{.....2.22}$$

$$L_{bsbs} = \frac{\mu_0 rl}{gp}\int_0^{2\pi}(N_B\cos(\varphi))^2 d\varphi = \frac{\mu_0 rl}{gp}\pi N_B^2 \quad \text{.....2.23}$$

$$L_{arar} = \frac{\mu_0 rl}{gp}\int_0^{2\pi}(N_r\cos(\varphi - \varphi_r))^2 d\varphi = \frac{\mu_0 rl}{gp}\pi N_r^2 \quad \text{.....2.24}$$

$$L_{arbr} = \frac{\mu_0 rl}{gp}\int_0^{2\pi} N_r\cos(\varphi - \varphi_r) \times N_r\sin(\varphi - \varphi_r)\, d\varphi = 0 \quad \text{.....2.25}$$

$$L_{brar} = \frac{\mu_0 rl}{gp}\int_0^{2\pi} N_r\sin(\varphi - \varphi_r) \times N_r\cos(\varphi - \varphi_r)\, d\varphi = 0 \quad \text{.....2.26}$$

$$L_{brbr} = \frac{\mu_0 rl}{gp}\int_0^{2\pi}(N_r\cos(\varphi - \varphi_r))^2 d\varphi = \frac{\mu_0 rl}{gp}\pi N_r^2 \quad \text{.....2.27}$$

$$L_{asar} = \frac{\mu_0 rl}{gp}\int_0^{2\pi} N_A\cos(\varphi) \times N_r\cos(\varphi - \varphi_r)\, d\varphi = \frac{\mu_0 rl}{gp}\pi N_A N_r\cos(\varphi_r) \quad \text{.....2.28}$$

$$L_{asbr} = \frac{\mu_0 rl}{gp}\int_0^{2\pi} N_A \cos(\varphi) \times N_r \sin(\varphi - \varphi_r)\, d\varphi = \frac{\mu_0 rl}{gp}\pi N_A N_r \sin(\varphi_r) \quad \text{.....2.29}$$

$$L_{bsar} = \frac{\mu_0 rl}{gp}\int_0^{2\pi} N_B \sin(\varphi) \times N_r \cos(\varphi - \varphi_r)\, d\varphi = \frac{\mu_0 rl}{gp}\pi N_B N_r \sin(\varphi_r) \quad \text{.....2.30}$$

$$L_{bsbr} = \frac{\mu_0 rl}{gp}\int_0^{2\pi} N_B \sin(\varphi) \times N_r \sin(\varphi - \varphi_r)\, d\varphi = \frac{\mu_0 rl}{gp}\pi N_B N_r \cos(\varphi_r) \quad \text{.....2.31}$$

Equation 2.6 – 2.8 become

$$L_s = \begin{bmatrix} L_{las} + L_{ma} & 0 \\ 0 & L_{lbs} + L_{mb} \end{bmatrix} = k \times \begin{bmatrix} N_A^2 & 0 \\ 0 & N_B^2 \end{bmatrix} + \begin{bmatrix} L_{las} & 0 \\ 0 & L_{lbs} \end{bmatrix} \quad \text{.....2.32}$$

$$L_r = \begin{bmatrix} L_{lr} + L_{mr} & 0 \\ 0 & L_{lr} + L_{mr} \end{bmatrix} = k \times \begin{bmatrix} N_r^2 & 0 \\ 0 & N_r^2 \end{bmatrix} + \begin{bmatrix} L_{lr} & 0 \\ 0 & L_{lr} \end{bmatrix} \quad \text{.....2.33}$$

$$L_{sr} = \begin{bmatrix} L_{asar} & L_{asbr} \\ L_{bsar} & L_{bsbr} \end{bmatrix} = k \times \begin{bmatrix} N_A N_r \cos(\varphi_r) & -N_A N_r \sin(\varphi_r) \\ N_B N_r \sin(\varphi_r) & N_B N_r \cos(\varphi_r) \end{bmatrix} \quad \text{.....2.34}$$

$$where k = \frac{\mu_0 rl}{g}\pi.$$

In Equation 2.32 and 2.33, the leakage inductances of the a-phase and b-phase stator windings are $L_{las} and L_{lbs}$ respectively, while those of the rotor windings is L_{lr}.

4. Simulation of the dynamic responds of Two-phase Induction Motor (TPIM) and Single-phase Capacitor Start and Capacitor Run Induction motor (CSCR-SPIM):

The considered TPIM and CSCR-SPIM design parameters are given in table 1

Table 1: Machines data for TPIM and CSCR-SPIM;

TPIM Parameters		CSCR-SPIM	
$L_{ls} = 0.002H$	Moment of inertia, J=0.015;	$L_{ls} = 0.002H$	Moment of inertia, J=0.015;
$L_{lS} = 0.002H$	No. of main turn N_a=34;	$L_{lS} = 0.002H$	No. of main turn N_a=40;
$L_{lr} = 0.0015H$	No. of auxiliary turn N_b=34;	$L_{lr} = 0.0015H$	No. of auxiliary turn N_b=28;
$L_{lR} = 0.0012H$	Rotor turns N_r=33;	$L_{lR} = 0.0012H$	Rotor turns N_r=33;
$r_{as} = 2.52\ Ohms$	No. of poles, p=4;	$r_{as} = 1.02\ Ohms$	No. of poles, p=4;
$r_{bs} = 2.52\ Ohms$	Effective stack length, l=0.15;	$r_{bs} = 4.028\ Ohms$	Effective stack length, l=0.15;
$r_{ar} = 4.12\ Ohms$	Air-gap radius, R=0.099	$r_{ar} = 4.12\ Ohms$	Air-gap radius, R=0.099
$r_{br} = 4.12\ Ohms$	Mu=4*pi*10^-7	$r_{br} = 4.12\ Ohms$	Mu=4*pi*10^-7

The simulated model was analyze and compared with symmetrical stator windings capacitor start capacitor run single-phase induction machine. The embedded MATLAB/Simulink block is shown in fig 2.

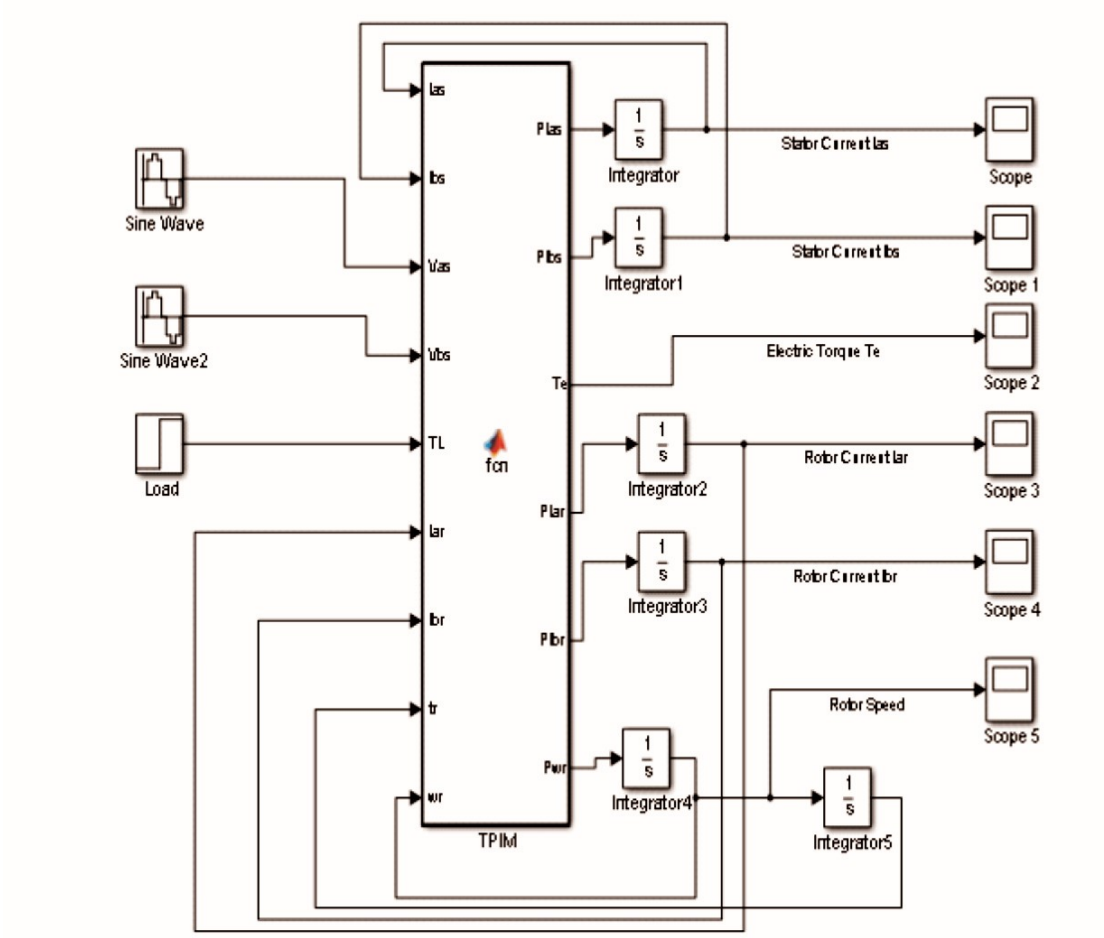

Fig. 2. Simulink model of the TPIM with two symmetrical windings and CSCR-SPIM.

5. Simulation Results.

The MMF distribution of TPIM is calculated using MATLAB. The number of turns in stator slots is calculated and the results areas shown in fig 3. The MMF distribution in the air gap is determined by the number of slots and the turns in each slot. A THD of 0.2173 for both windings. is recorded.

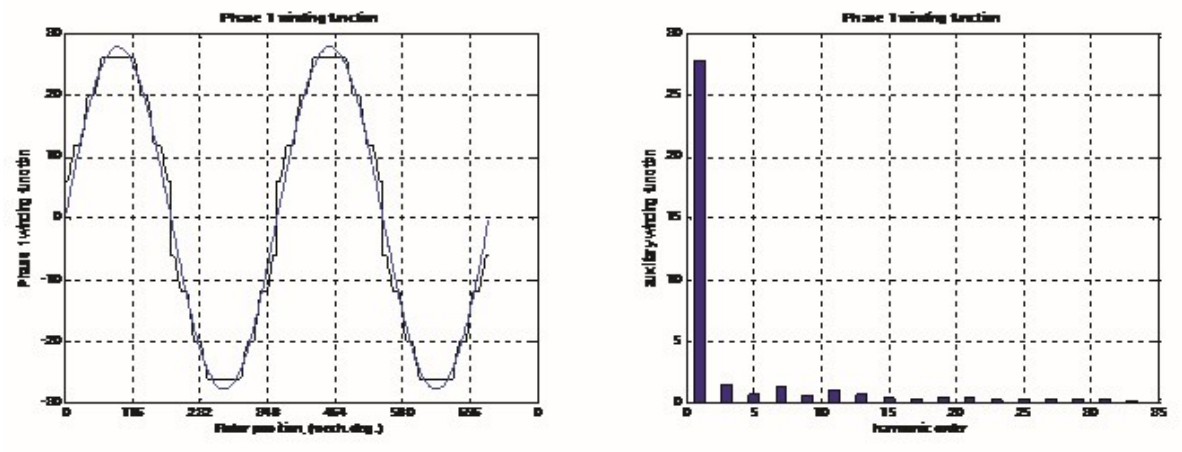

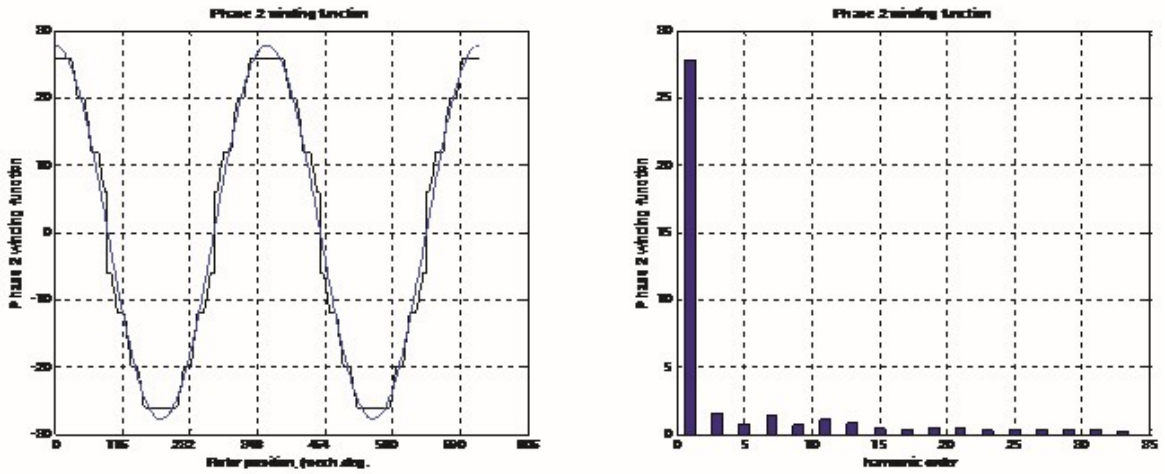

Figure 3: Plot of Winding function diagram and Harmonic order for phase A and B of TPIM.

5.2: Simulation waveforms for TPIM at no-load and 10Nm load condition:

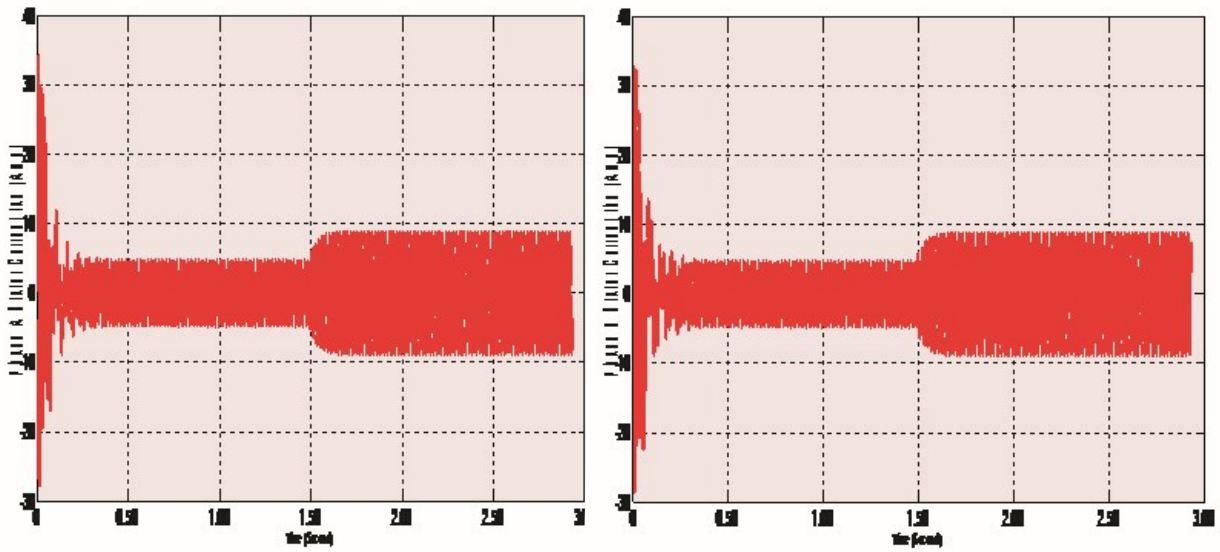

Fig. 4. Phase A and B Stator Current for Two-Phase Induction Motor (TPIM) with two symmetrical windings showing starting, no-load and 10Nm load current.

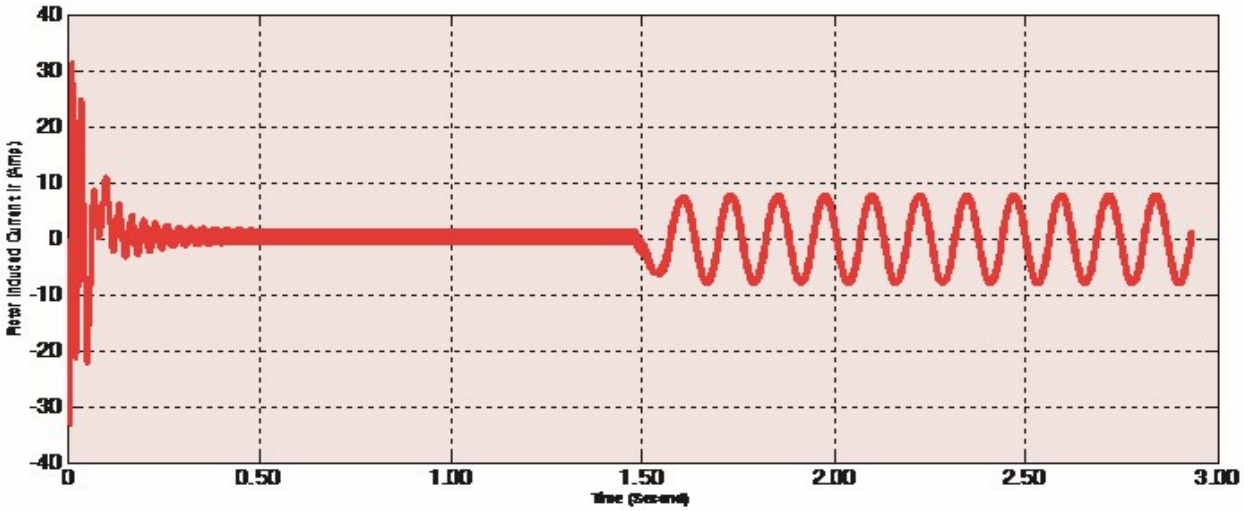

Fig.5. Rotor Induced Current l_{ar} and l_{br} for TPIM is the same at no-load and load condition.

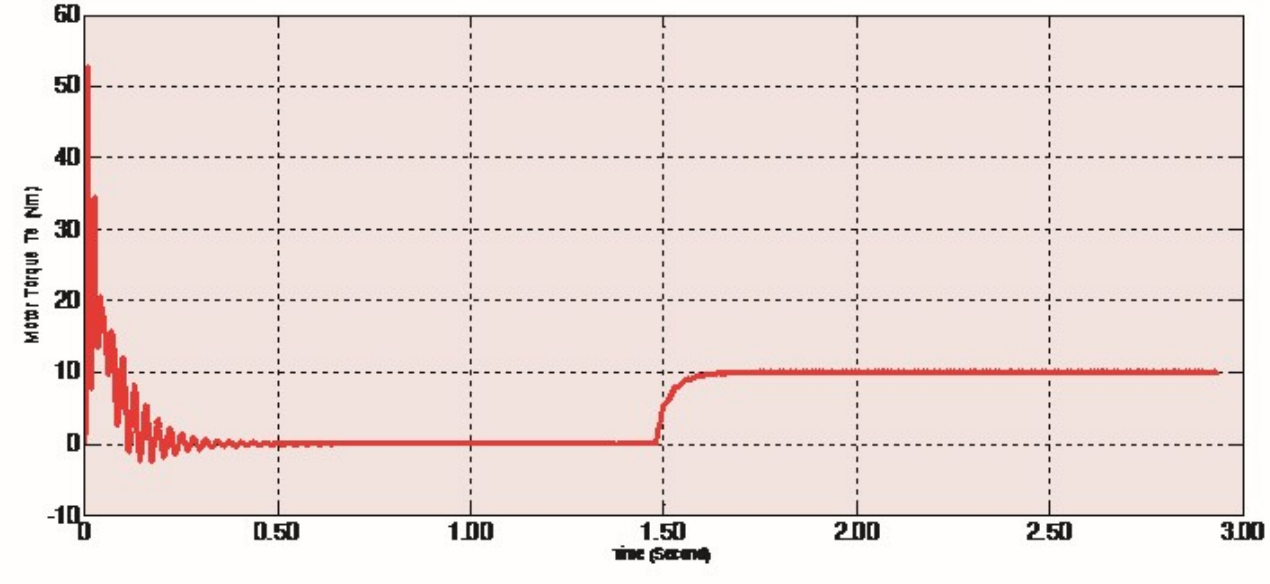

Fig.6. Electromagnetic Torque developed by the TPIM showing transient and steady state condition.

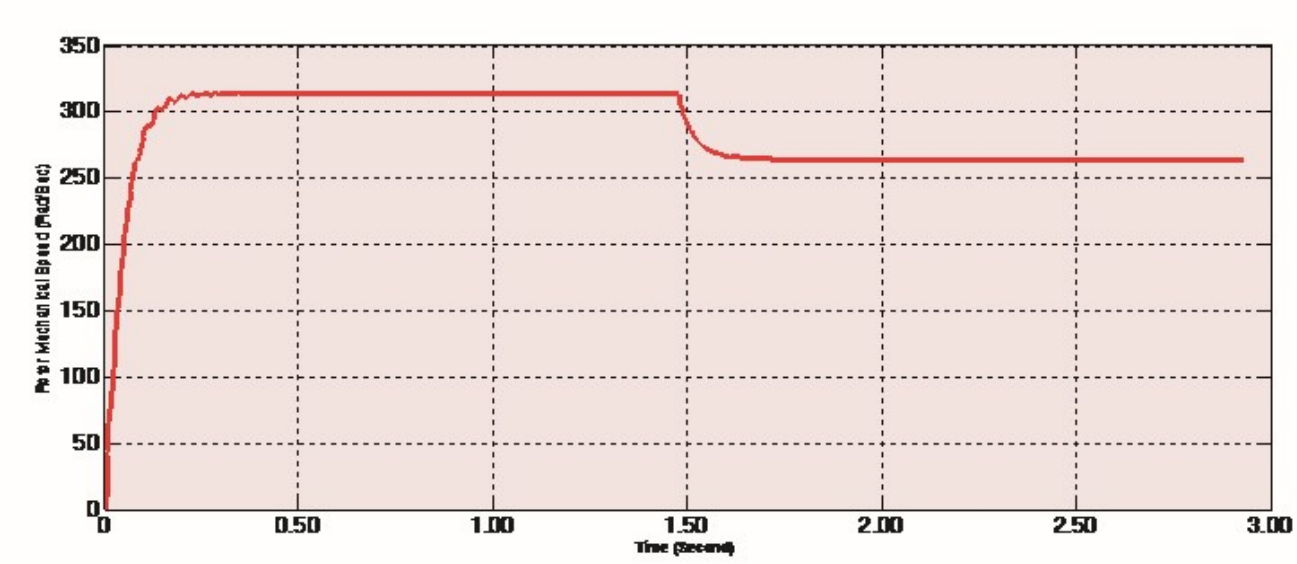

Fig.7. Rotor Mechanical Speed for the TPIM showing no-load and load speed.

5.3: Simulation waveforms for CSCR-SPIM at no-load and 10Nm load condition:

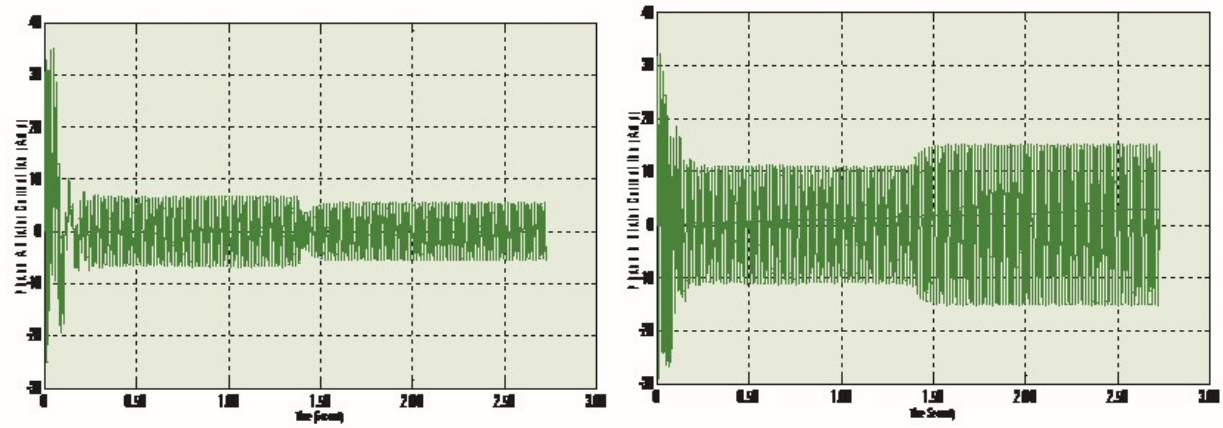

Fig. 8. Phase A and B Stator Current for CSCR-SPIM showing starting, no-load and 10Nm load condition.

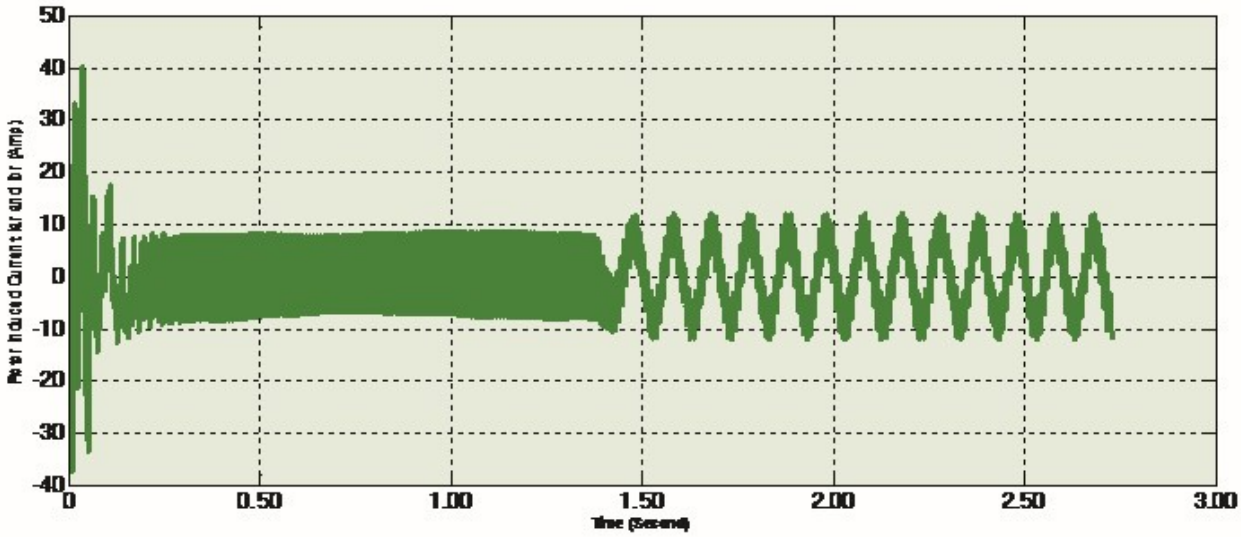

Fig.9. Rotor Induced Current I_{ar} and I_{br} for CSCR-SPIM is the same during starting, no-load and at 10Nm load.

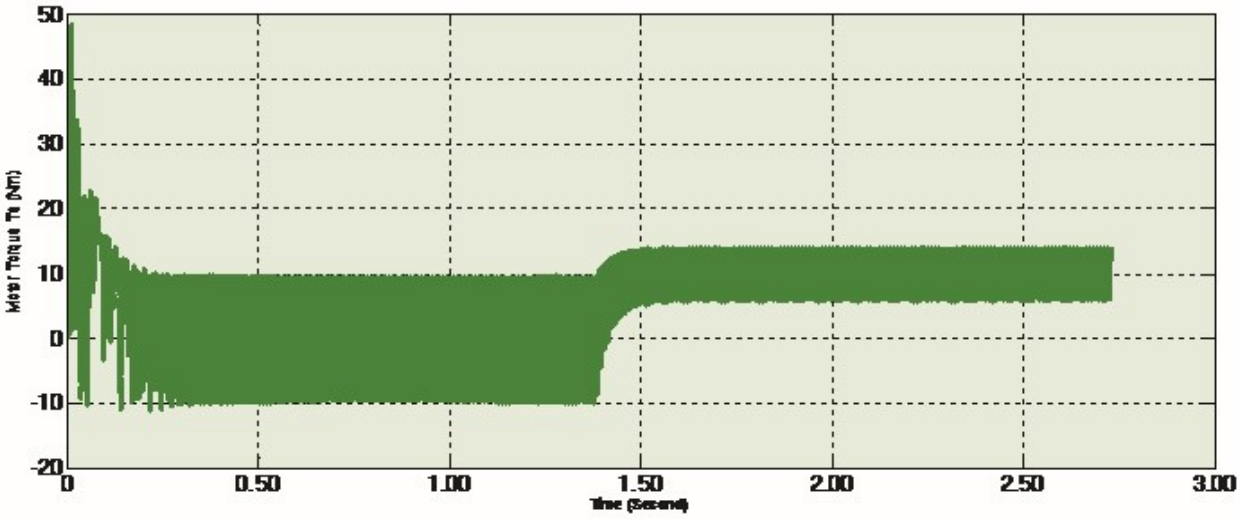

Fig. 10. Electromagnetic Torque developed by the CSCR-SPIM showing transient variation.

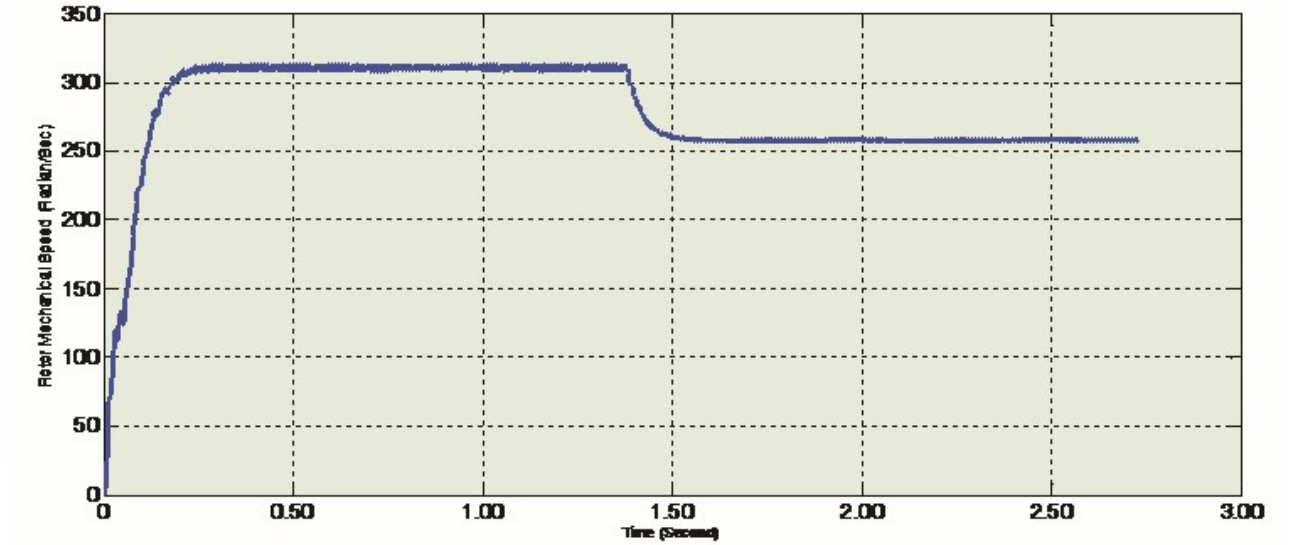

Fig. 11. Rotor Mechanical Speed for the CSCR-SPIM showing no-load and load speed.

Figure 4 - 11 shows the transient and steady state variables for phase A and B stator current $_{as}$and$_{ibs}$ rotor induced current torqueT_e characteristic at no-load and load condition for two-phase induction motor TPIM and CSCR-single-phase induction motor simulation.

Table 2: The simulation results for TPIM and CSCR-SPIM.

Motor	Conditions	Stator Current b/w Phase A&B	Rotor Induced Current	Motor Torque	Motor Speed
TPIM	Max. Starting Current; No-load Current; Load Current (10Nm);	A&B-34.25A A&B- 4.25A A&B- 8.00A	34.25A 1.60A 7.80A	52.8Nm 0.1Nm 10.1Nm	313rad/s 316rad/s 265rad/s
CSCR-SPIM	Max. Starting Current; No-load Current; Load Current (10Nm);	A- 35, B - 32.2A A- 7.7, B - 11.0A A- 5.0, B - 15.0A	40.0A 8.5A 12.0A	48.5Nm 10.0Nm 15.0Nm	311rad/s 308-313 255-259

5.4: Stator and Rotor Induced Current

Fig 4 and 8 shows the TPIM main and auxiliary stator current waveform for maximum starting current of 34.25A, no-load steady state current of 4.5A and 10Nm load current of 8A plotted against time. The TPIM rotor induced current is nearly equal to the amount of current flowing in the stator winding during startup transient. These current dropped to 1.6A at no-load steady state operation, and when a load of 10Nm applied, it drew 8A. Comparatively, the CSCR-SPIM main and auxiliary stator winding drew current of 7.7A and 11A at no-load steady state operation. But when a load of 10Nm applied, the main phase current dropped to 5A while auxiliary drew 15A respectively. These imbalances in current are due to phase winding difference, these causes more current to go through the B phase which obviously produced radial force on the rotor.

5.5: Electromagnetic torque:

Fig 6 and 10 shows the electromechanical torque developed by the two machines; the TPIM have higher starting torque of 52.8Nm as compared to 48.5Nm produced by the CSCR-SPIM. At no-load, a current of 4.23A is drawn by the stator winding which causes 1.6A to be induced on the rotor bars. This small current causes mechanical torque of 0.1Nm to develop on the rotor. On application of 10Nm load, the TPIM drew 7.8A to generate nearly equal amount of electric torque required to drive the load smoothly. Meanwhile, the CSCR-SPIM draws unequal no-load current of 7.7A and 11A, and induced in the rotor a maximum of 8.5A. This two current built up inductance of different values in the air-gap and causes the rotor torque to oscillate or ripples during no-load operation. But during load operation, the CSCR-SPIM drew 15A to drive a 10Nm load with the pulsating torque.

5.6 Rotor Speed:

Fig 7 and 11 shows the relationship between the rotor speed and time, the transient respond and steady state operation for TPIM and CSCR-SPIM. The two-phase induction motor speed reached a peak value of about 313rad/sec at 0.012 second before it stabilized to 316rad/sec at 0.025 second. The single-phase induction motor attained it maximum speed of 308rad/sec at 0.04 second and ripple between 308rad/sec to 313rad/sec at no-load steady state.

Fig. 7 shows a balanced current of 4.5A at steady as a result of equal number of turns in the TPIM. Fig 11 shows unequal distribution of current between the main (phase B) and auxiliary (phase A) winding as a result unbalanced winding resulted in higher current of 11A at steady state operation. Fig 7 and fig 11 shows that the two motors exhibited nearly equal electromagnetic torque at transient state.

5.7 Load condition

In this paper, a load of 10 Nm was introduced at 1.5 second. The behavior of the two motor was monitor as shown in fig 4 - 11. The stator current rises to 8A in two-phase motor while that single-phase motor recorded 15A. Expectedly, the rotor speed in both motor dropped to 255rad/sec and ripples significantly in the SPIM as shown in fig 7 and 11. The electromagnetic torque increases in order to accommodate the load torque. The torque developed in the two-phase motor seen to be higher than the single-phase counterpart. In SPIM, the rotor torque pulsates at steady state and increase significantly with load than the two-phase motor.

6. CONCLUSIONS

This paper proposed a single-phase induction motor with two symmetrical windings driven with two-phase power supply. The proposed configuration granted SPIM the advantages of multiphase machines such as heavy starting torque, high efficiency, higher rated power etc. The currents, torque and speed analysis of the motor performance were reported. The results confirmed that TWO-PHASE-IM mode of operation provided better performance than CSCR-SPIM. The motor features such as; low inrush current; the

increased output per current which impact significantly in the running cost in term of volt-ampere, with reduction on watt per hour cost. It runs smoothly as indicated in the plot of the rotor speed, with little or no ripples, which invariably would have affected the bearing at long run, noise reduction is of essence, and an additional advantage.

7. REFERENCES

Naser Abdel-Rahim & Adel Shaltout (2002). Operation of Single-phase Induction Motor as Two-
phase Motor. *The 28th ANNUAL Conference of the IEEE industrial Electronics Society,* 2.

https://doi.org/10.1109/IECON.2002.1185403

Sobhan Sobhani, Hamid Yaghobi & Mehdi Samakoosh (2013). Optimize Efficiency and
Torque in the Single-phase Induction Motor by Adjusting the Design Parameters, *IEEE*
Environment and Electrical Engineering Conference, EECIC 12th international conference.

https://doi.org/10.1109/EEEIC.2013.6549623

Hraboveova, V., Kalamen, L., Sekerak, P., & Rafajdus, P. (2010). Determination of single-
phase motor parameters, *IEEE Power Electronic Electrical Drives Automation and Motor*
(SPEEDAM) international Symposium, https://doi.org/10.1109/SPEEDAM.2010.5545087

Mera, R., & Campearu, R. (2012). Optimal Performances of Capacitor-Run Single-Phase
Induction Motor, *13th International Conference on Optimization of Electrical and Electronic*
Equipment, IEEE Transaction, https://doi.org/10.1109/OPTIM.2012.6231966

Huang, H., Fuchs, E., & White, J. (1988). Optimal Placement of the Run Capacitor in Single-Phase
Induction Motor Designs, *IEEE Transaction on Energy Conversion, 3*(3), 647-652.
https://doi.org/10.1109/60.8080

Fushs, E., Vandenput, A., Holl, J., & White, J. (1990). Design Analysis of Capacitor-Start
Capacitor-run Single-phase Induction Motors*, IEEE Transaction on Energy Conversation, 5*(2).
https://doi.org/10.1109/60.107229

Zhou, P., Scott, S., & Cendes, Z. (1999). Dynamic Modelling of three-Phase and Single-Phase
Induction Motors," *Electrical Machines and Drives 1999. International conference IEMD'99*.
Seattle, WA. https://doi.org/10.1109/IEMDC.1999.769174

Xinhua, L., Hao, X., & Keding, Z. (2001). Starting Process Simulation of Nd-Fe-B single-phase
Permanent-Magnet Synchronuos Motor Fed by PWM Inverter, *IEEE Electrical Machines and*
Systems, 2001. ICEMS 2001 Proceedings of the Fifth International Conference on, 2.

https://doi.org/10.1109/ICEMS.2001.9718117

Vishal, V., Peeyush, P., & Bhim, S. (2008). Simulation of a Single-phase Induction Motor
with Dynamic Capacitor for Maximum Torque Operation*, IEEE Power India Conference 2008,*
Power System Technology conference. https://doi.org/10.1109/ICPST.2008.4745291

Sorrentino, E., & Fernandez, S. (2011). Comparison of six steady-state models for single-
phase induction motors, *Published in IET Electric Power Applications*, *5*(8). 611- 617
https://doi.org/10.1049/iet-epa.2011.0001

Van der Merwe, C., & van der Merwe, F. (1995). A Study of Methods to Measure the Parameters
of Single-phase Induction Motors, *IEEE*

Transaction on Energy Conversion, 10(2). 248-253
https://doi.org/10.1109/60.391889
Salon S. J. (1995). *Finite Element Analysis of Electrical Machines"*.Kluwer Academic Publishers.
July, 1995 Edition
Vassent, E., Meunier, G., & Foggia, A. (1991). Simulation of induction machines using complex
magnetodynamic finite element method coupled with the circuit equations, ***IEEE, Transactions*** *on* ***Magnetics,*** *27*(5). 4246-4249 https://doi.org/10.1109/20.105039